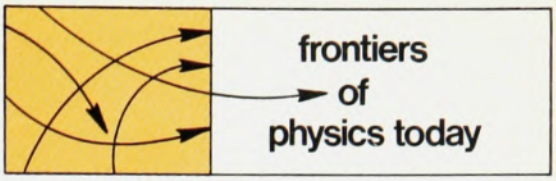

Ultrafast laser pulses

These powerful pulses occur quickly enough to reveal transient details of such phenomena as fluorescence decay, stimulated Raman scattering and plasma formation.

Anthony J. DeMaria, William H. Glenn and Michael E. Mack

By "ultrafast" we mean those light pulses that last from about 10^{-13} seconds to a few tens of picoseconds. The anticipation of using them to study ultrafast processes in physics and chemistry has stimulated efforts to produce these pulses, and the results have been good; in 1962 the shortest pulse available was 10^{-8} sec,[1] but by 1968, 10^{-13}-sec pulses had been produced at powers up to 10^{12} watts.[2] Progress has been due largely to the perfection of "mode-locking" methods, through which we arrange the phase relations between the axial modes of the laser. Here we shall discuss the ways ultrafast pulses are produced and measured. Then we can consider their usefulness in, for example, studying stimulated scattering, measuring excited-state lifetimes and creating high-temperature plasmas.

Before we go further, note that the 10^{-13}-sec limit is theoretically determined by the spectral bandwidth of the laser chosen to generate the pulse. The neodymium-glass laser is usually preferred because of its large bandwidth, and by 1967, early in the history of ultrafast-pulse generation, indirect measurements with interferometers and spectrometers[3] had already found a lower limit on its pulse duration.

Anthony DeMaria, William Glenn and Michael Mack are all with United Aircraft Research in East Hartford, Conn., where DeMaria is chief physicist of the Electromagnetics Laboratories. Glenn is Principal Scientist and Mack is Senior Research Scientist in the Quantum Physics Group, which is a part of the Electromagnetics Laboratories.

Generating the pulses

If we think of a laser as a resonant Fabry–Perot cavity, large compared with the oscillating wavelength emitted by the active optical medium it contains, we see that many axial interferometer resonances (modes) within the laser linewidth can oscillate more or less independently of one another. These

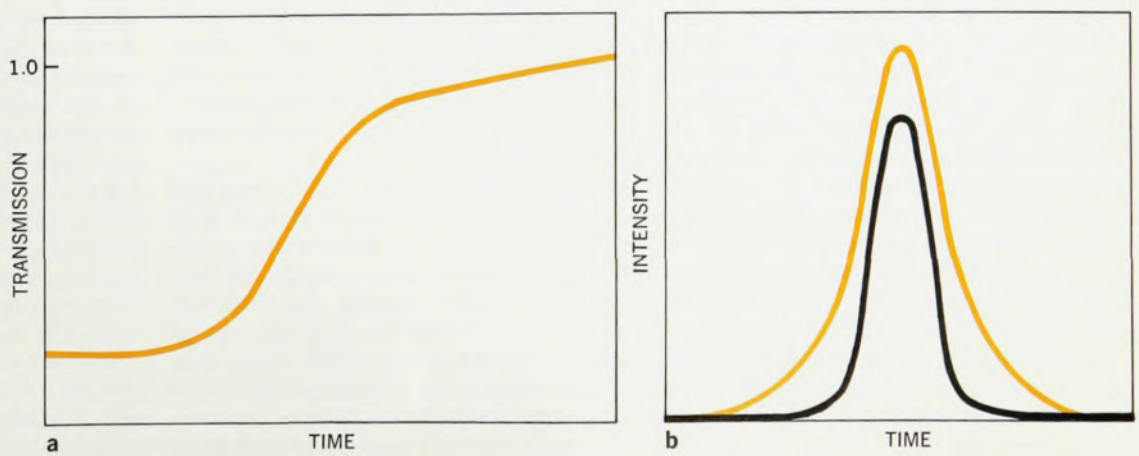

Saturable absorbing dye. Because the dye attenuates higher amplitudes less than lower amplitures (a) it acts as a passive modulator, and an input pulse (color) is "sharpened" (b) into an ultrafast pulse (black). Figure 1

modes are, in general, uncoupled and have no fixed phase relationship with one another.

To generate ultrafast pulses, we must couple together several of the laser modes. Either an "active" externally driven modulator such as a signal generator, or a "passive" modulator such as a saturable dye, can be used to achieve the needed mode relationships. If we put an active modulator, operating at a frequency f_l, into the laser's feedback path, and the mode υ_m nearest the peak of the laser gain profile begins to oscillate, υ_m will develop sidebands at $\upsilon_m \pm f_l$. If we choose the modulating frequency f_l to be equal to the separation f between the laser's axial mode frequencies, the upper ($\upsilon_m + f_l$) and lower ($\upsilon_m - f_l$) sidebands will couple with the adjacent axial modes with a well defined amplitude and phase. As the sidebands pass through the modulator they too will be modulated, and the mode-coupling process will continue across the entire inverted spectral line of the laser. The laser is now said to be "mode locked."[4]

Mode-locked lasers can have high peak powers, because the power contained in the entire output of the uncoupled laser is now contained within the more intense ultrafast pulses. We see this if we think of the constructive and destructive interference of the phase-locked modes in terms of the interference of Fourier components in the construction of a repetitive pulse train. The time interval τ between the repetitive pulses is equal to $1/f$; if there are n modes the pulsewidth equals $1/nf$ or $(1/n)\,\tau$. The ratio pulse-on-to-pulse-off (the "duty cycle") then equals $1/n$, so that the peak power of the pulse is n times the average power. For a neodymium-glass laser, n can be as high as 10^4.

Active mode locking is fairly well understood, and we find that theory and experiment agree. Passive mode locking with a saturable dye is, despite its wide use, less well understood, but we can give some qualitative understanding of the evolution of an ultrafast pulse from a saturable dye that has the transfer characteristics shown in figure 1, and a neodymium-glass laser. The pumping starts and gives rise to a growing population in the upper laser level. The excited atoms radiate spontaneously, and the spectral width of the radiation increases as more of the inhomogeneous linewidth is excited. After about a millisec, the "small-signal" threshold is reached; that is, the gain in the cavity is equal to the loss in the "unbleached" dye. The radiation field in the cavity now consists of a noiselike signal with a spectral content of about 200 cm^{-1} and amplitude fluctuations in a time scale of a few tenths of a picosecond.

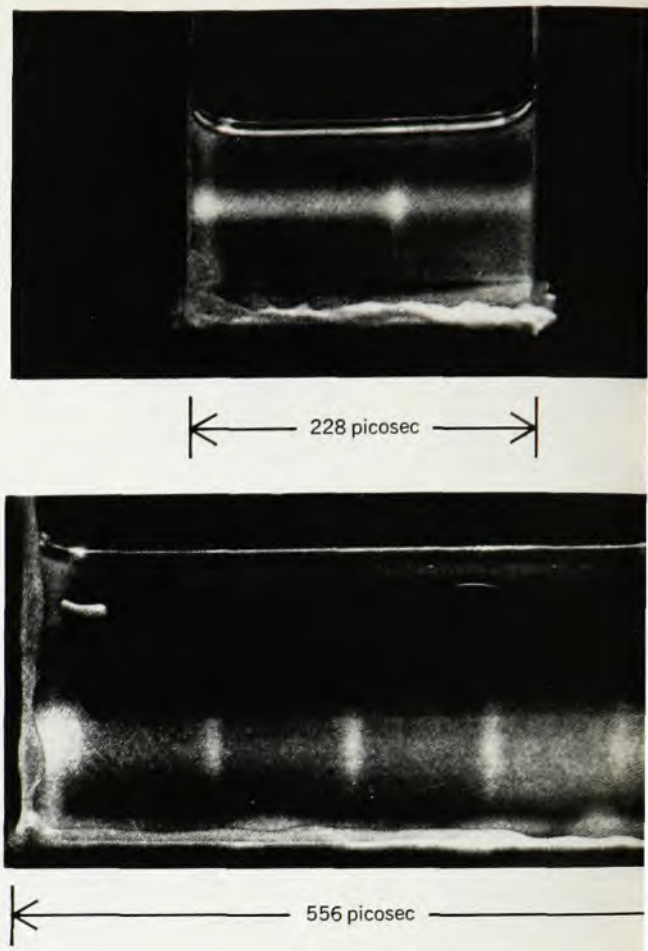

Two-photon absorption method measures the duration of an ultrafast pulse. The laser beam is passed through a dye that has a two-photon absorption peak at the laser frequency and is reflected back on itself. A series of equally spaced bright spots then appears along the beam path; their width is a measure of the pulse duration. Figure 2

As time goes on the gain increases above threshold, and the noiselike signal is amplified. As a result of the finite bandwidth of the amplifier, successive passes through the cavity reduce the spectral width of the signal and increase the time scale of the random amplitude fluctuations to several picoseconds. Eventually the intensity of the signal is great enough to begin saturating the dye; this occurs at a power of about 50 MW/cm^2.

The nonlinear response of the dye now becomes important. The dye attenuates higher-amplitude pulses less than lower-amplitude pulses, and under the proper conditions of dye transmission, pumping rate and linear loss, the random signal evolves into a signal consisting of an isolated fast pulse that can be traced back to one of the larger random amplitude fluctuations present initially. During the evolution the pulse undergoes some shortening as a result of the nonlinearity, and the spectral width increases.

Eventually the pulse is so intense that the dye becomes saturated and ineffective, and we may get another period of linear amplification until the laser amplifier itself begins to saturate. There are indications that as the intensity of the pulse grows other nonlinear forces (such as nonlinearity in the laser glass rod) come into play, impressing an amplitude and phase substructure on the pulse. As a result the fully developed pulse has a spectral width of 100–200 cm^{-1}, about ten times as wide as expected for a pulse a few picoseconds long. Finally the laser gain is depleted and the pulse decays.

Measuring ultrafast pulses

The duration of relatively long (down to about 150 picosec) optical pulses is usually measured as an oscilloscope display of the output of a photodetector illuminated by the pulse. But direct electronic measurements of picosecond pulses can not be made, and measuring techniques had to be invented.

Linear optical instruments, such as interferometers and spectrometers,[3,5] had been able to find the limit on the shortness of the pulses but were incapable of measuring the pulses directly. Appropriate nonlinear optical instruments that measure the autocorrelation of the pulse intensity can provide information about the actual duration of a pulse[5,6]; to date these instruments have used second- and third-harmonic and two- or three-photon absorption methods. Because two-photon absorption is simple and more widely used than the optical-harmonic method, we shall discuss it in some detail.

In the two-photon absorption method, the output of the laser passes through a cell containing a highly fluorescent dye that has a two-photon absorption peak

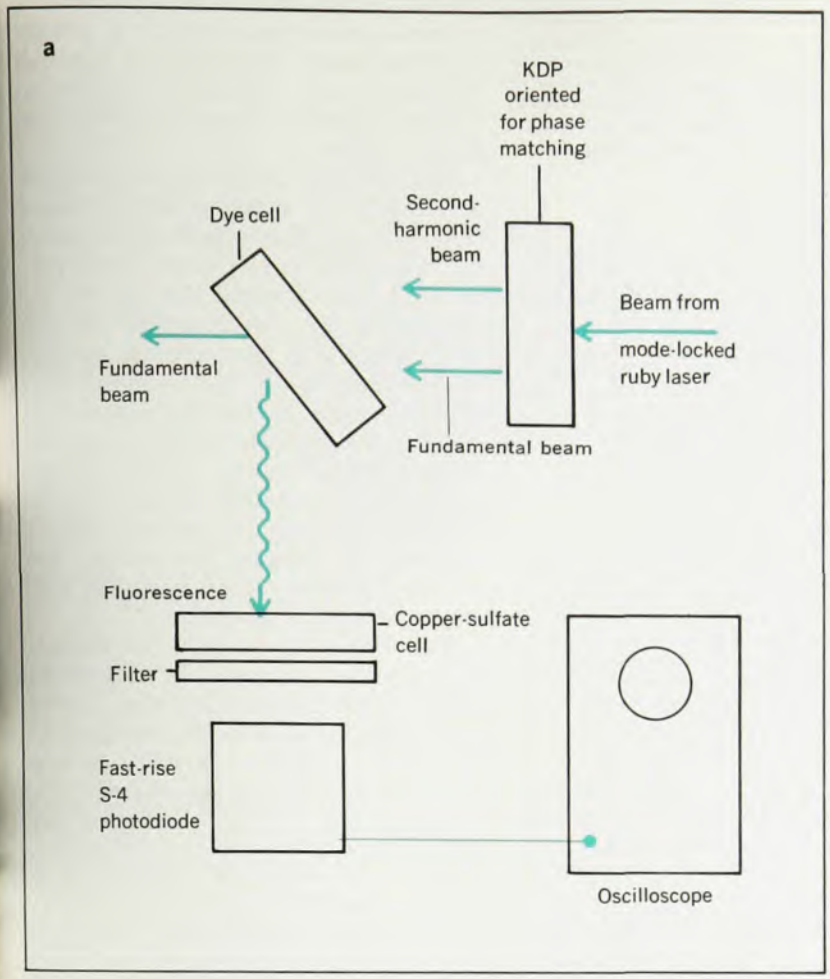

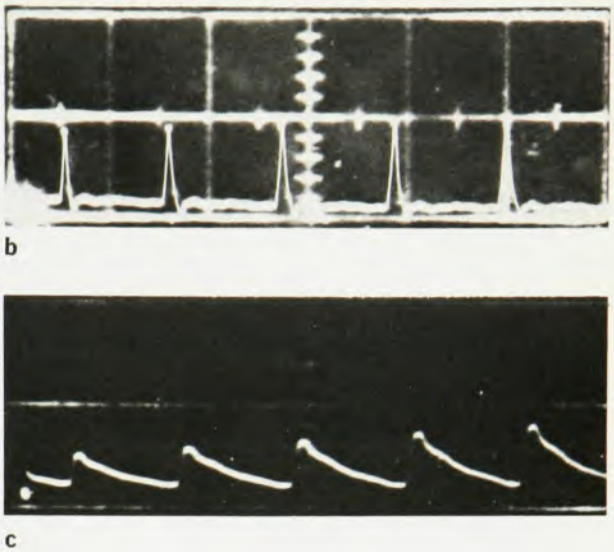

Fluorescence decay in an organic dye is studied with an experimental arrangement (a) that includes a traveling-wave oscilloscope and a fast-rise photodiode. An oscilloscope photograph of the laser output (b) shows the time resolution of the system (scale here is ten nanosec per division); the fluorescence signal (c) is observed directly on the oscilloscope screen.
Figure 3

at the laser frequency. A molecule can be excited from the ground state either by absorbing a single photon of a suitable frequency ω_1, or by the simultaneous absorption of two photons with frequency $\omega_2 = \omega_1/2$, even though there is no real intermediate state of the molecule corresponding to ω_2. Unless two photons are available simultaneously, however, absorption and subsequent fluorescence at a frequency ω_F (where $\omega_2 < \omega_F < \omega_1$) does not occur.

We place a mirror at the end of the dye cell opposite to the entrance of the laser beam to reflect the beam back on itself. Because the fluorescent intensity is proportional to the square of the laser intensity, a series of equally spaced bright fluorescent spots, shown in figure 2, occurs along the path of the laser beam, corresponding to the superposition of the pulses traveling in opposite directions. The width of these fluorescence spots is a measure of the length of the light pulses, provided the ratio of intensity of the fluorescence spot to the background is three to one; a high-intensity noise pulse of the proper duration and bandwidth would give similar spots, but the spots then would be only one and one half times as intense as the background.

Some applications

The very short duration and high peak power of pulses from mode-locked lasers suit them ideally for studying physical and chemical processes that take place in the 10^{-9} to 10^{-13}-sec time scale. These processes have until now been amenable only to indirect observations. We can get an idea of the range of the advances made with ultrafast pulses by discussing a few specific applications.

Molecular-lifetime studies. Fluorescence decay is the simplest type of lifetime measurement. Fluorometers able to measure lifetimes less than a nanosecond have been available since the early 1930's,[7] but they are complex and cumbersome. They have the disadvantage that, because the actual decay curve is not observed, the measurements are indirect and subject to interpretation. By using high peak-power mode-locked lasers to excite the fluorescence under study, we can get simple and direct fluorescence-decay time measurements.

Of the lasers that have been successfully mode locked, the pulsed neodymium–glass and ruby lasers offer the greatest peak power. For materials that absorb in the blue rather than the red end of the spectrum, these lasers can be used along with frequency doublers. Alternatively, we can use a tunable mode-locked dye laser.[8] Argon lasers as well as neodymium:yttrium–aluminum–garnet (Nd^{3+}:YAG) lasers provide continuously mode-locked outputs suitable for lifetime measurements.

If we use the continuously mode-locked lasers, together with crossed-field photomultipliers and sampling oscilloscopes, we can study rise times as short as 60 picosec. With the pulsed mode-locked lasers, however, we must use traveling-wave oscilloscopes, which typically have rise times of the order of tenths of a nanosecond.

Fluorescence decay studies with traveling-wave oscilloscopes and fast photodiodes have recently been carried out for a number of organic dyes with mode-locked ruby lasers[9] in an experimental arrangement like the one in figure 3a. Figure 3b is an oscilloscope photograph of the laser output and shows the time resolution of the system; the scale is 10 nanosec per division. The signal produced by the fluorescing dye is shown in figure 3c. Decay measurements made from photographs such as this one are accurate to better than 20%.

A novel use of the optical Kerr effect overcomes the limitations of the electronic monitoring equipment with a new kind of Kerr shutter.[10] The mode-locked laser beam both excites the fluorescence and, through the optical Kerr effect, operates the shutter. The sample fluorescence is observed through the shutter, and by monitoring the observed signal as a function of the delay time between the fluorescence excitation and the shutter-opening time, we determine the decay time. With this

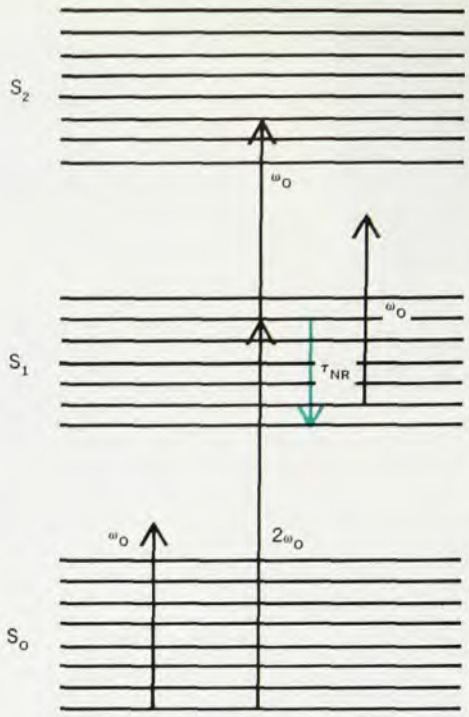

Energy levels in azulene. Second-harmonic radiation ($2\omega_0$) of a mode-locked neodymium–glass laser excites a ground-state molecule to an excited sublevel in the first excited-singlet band, from which it decays nonradiatively in a time τ_{NR}. The more intense fundamental radiation (ω_0) can excite the molecule to the second-excited singlet (from which the molecule fluoresces) only if the molecule is already in an excited sublevel. Varying the delay between the fundamental and second-harmonic beams has shown that τ_{NR} equals 7.5 picosec.
Figure 4

device, Michel Duguay and John Hansen have measured[11] the fluorescence decay times of two ruby-laser mode-locking dyes, "DDI" and cryptocyanine, to be 14 ± 3 and 22 ± 4 picosec. They have also used the optical Kerr shutter system to investigate rotational relaxation in molecules that have an anisotropic polarizability.

For saturable absorbing dyes we have an alternative way to determine lifetimes. If the dye absorbs a very intense picosecond light pulse, the ground-state population is considerably reduced. Consequently a much weaker pulse incident on the dye a short time later will be absorbed less than the original pulse. As the delay time between the saturating pulse and the probing pulse is increased, the population will relax back to the ground state, and the probing-pulse absorption will increase. With this method, the decay times for Eastman 9740 and 9860 dyes have been found to be about 35 and 9 picosec.[12] Kenneth Eisenthal and K. H. Drexhage used a variation of the saturating-pulse probe[13] to investigate orientational relaxation of absorbing molecules in a liquid solution.

Picosecond laser pulses allow us to measure the nonradiative relaxation rate in a dye directly for the first time. Experiments have been done on the dye azulene,[14] whose energy-level scheme is shown in figure 4. Unlike most fluorescing dyes, azulene fluoresces from the second excited-singlet band S_2, but not from the first excited-singlet band S_1. The second harmonic $2\omega_0$ of the mode-locked neodymium-glass laser excites a ground state molecule to an excited sublevel of the first excited singlet. From there the molecule decays nonradiatively to the lowest level in the excited singlet with a decay time τ_{NR}. The more intense fundamental of the laser, ω_0, can not excite the molecule from the *lowest* sublevel of the first excited singlet to the second excited singlet, but it can excite the molecule as long as the molecule remains in the *excited* sublevel. The molecule decays by fluorescence from the second singlet. Varying the delay between the second-harmonic and fundamental beams has shown this relaxation time to be $\tau_{NR} = 7.5$ picosec.

Within the past year, Peter M. Rentzepis and his coworkers have reported[15] the direct observation of an ultrafast, time-resolved emission spectrum of a dye molecule in solution. They measure the vibrational relaxation time within the vibrational band of the excited state of rhodamine 6G as 6 picosec.

The molecular-kinetics experiments performed so far have shown the feasibility of the techniques involved. Nearly all have been carried out on liquid samples, but useful measurements should also be possible in gases and solids.

Stimulated scattering. Q-switched laser pulses lasting several tens of nanoseconds have been used to investigate a number of different stimulated scattering processes. These processes include Rayleigh scattering, Rayleigh wing scattering, Brillouin scattering and Raman scattering. With the exception of Brillouin scattering, the material excitation involved in the scattering process can follow the time variation of these relatively long laser pulses. Recently, stimulated thermal Rayleigh scattering and stimulated Raman scattering have been investigated in the transient limit with mode-locked laser pulses; with these shorter pulses the material excitation, which is a density or temperature fluctuation in Rayleigh scattering or a molecular vibration in Raman scattering, can not follow the pulse envelope.

Spontaneous Rayleigh scattering is associated with nonpropagating thermal fluctuations in the sample and is caused by variations in refractive index produced by the thermal fluctuations directly and by the resultant density fluctuations. In a transparent sample, light will not affect the thermal fluctuations strongly, so that stimulated Rayleigh scattering can not be produced. If the sample, however, is made slightly absorbing, the absorption provides the necessary coupling between the optical field and the thermal fluctuations, and we can observe stimulated Rayleigh scattering at high intensities.[16]

The origin of the gain in thermal Rayleigh scattering can be understood with the aid of figure 5, which shows two beams incident on the sample. In the overlap region an intensity grating forms in the sample because of interference. The refractive index of the sample depends on the beam intensity, leading to a refraction "grating" with such an orientation and periodicity as to scatter the stronger beam (say beam 1) into the direction of the weaker beam. The increased intensity in the direction of the weak beam further enhances the grating, increasing the scattering in its direction. Consequently, as the two beams cross the sample, the weak beam is amplified at the expense of the stronger beam.

Figure 6 brings out the grating nature of the gain effect quite clearly. Four beams are incident on the sample, two at the ruby-laser fundamental frequency ω_0 and two at the second-harmonic frequency $2\omega_0$. The second-harmonic beams are weak and the liquid solution does not absorb them. Consequently no stimulated thermal scattering is produced when the second-harmonic beams alone impinge on the sample. But the much more intense fundamental beams produce several orders of scattering (figure 6b) and, in the presence of the intense fundamental beams, the harmonic beams are also scattered (figure 6c). As expected from the grating model, the angular spacing of the orders for the harmonic-beam scattering is just half the spacing for the fundamental beam.

Forward thermal Rayleigh scattering has also been examined experimentally.[17,18] In these studies two beams, both from the same mode-locked ruby laser but one much less intense than the other, hit the absorbing sample at a slight angle with respect to each other. Several different scattering processes contribute to the observed weak-beam gain,[18] and to some extent the mode-

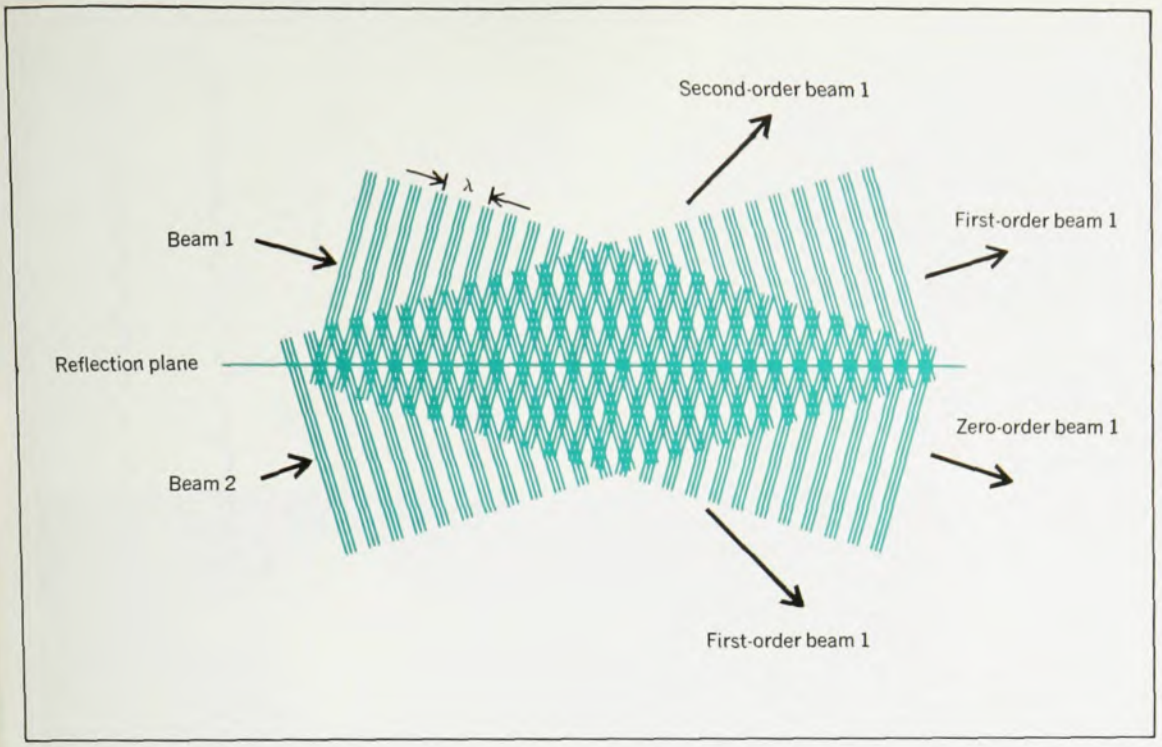

Intensity-grating model for origin of gain in thermal Rayleigh scattering. Two beams incident on a liquid sample form an "intensity grating" in their overlap region in such a way that the stronger beam (1) is scattered in the direction of the weaker beam (2), amplifying the weaker beam at the expense of the stronger. Figure 5

locked pulse train allows the separation of the different contributing effects by their different time responses.

Of all stimulated scattering processes, stimulated Raman scattering has received the most attention. The mechanism responsible for spontaneous Raman scattering is seen in figure 7. In Stokes scattering (decreasing in energy) the molecule is initially in its ground state. An incident photon at frequency ω_0 loses energy to the molecule and is scattered away at a lower frequency, leaving the molecule in an excited state. The molecular states involved are generally rotational or vibrational. If the molecule is already in an excited rotational or vibrational state the photon can gain energy from the molecule and be scattered at a higher frequency. The phenomenon is referred to as anti-Stokes (upward in energy) scattering (see figure 7). Here we are interested mainly in stimulated Stokes-type Raman scattering.

The characteristic response time in stimulated Raman scattering is, roughly speaking, the reciprocal of the spontaneous Raman linewidth. For those lines that have been stimulated, the linewidths range from about 0.1 cm^{-1} to 20 cm^{-1}, giving a characteristic time of 0.5 to 100 picosec. The short times indicate that, although the steady state is achieved in stimulated Raman scattering by *Q-switched* pulses, the scattering produced by *mode-locked* pulses of picosecond duration must be transient.

Theoretical treatments of transient stimulated Raman scattering[19] indicate that, in the transient limit, the gain is reduced, that the Stokes pulse narrows in time rather than in frequency, that it is delayed with respect to the laser pulse, and that the transient gain coefficient is proportional to the total integrated Raman cross section and independent of linewidth. These results contrast with the steady-state limit, in which the Stokes radiation is narrowed in frequency and the Raman gain coefficient is proportional to the ratio of the total Raman cross section to the Raman linewidth.

All of the theoretical predictions about transient stimulated Raman scattering have been verified experimentally. The transient gain coefficient is independent of the Raman linewidth, so that broad lines not stimulated with Q-switched pulses because of their low peak cross sections can often be stim-

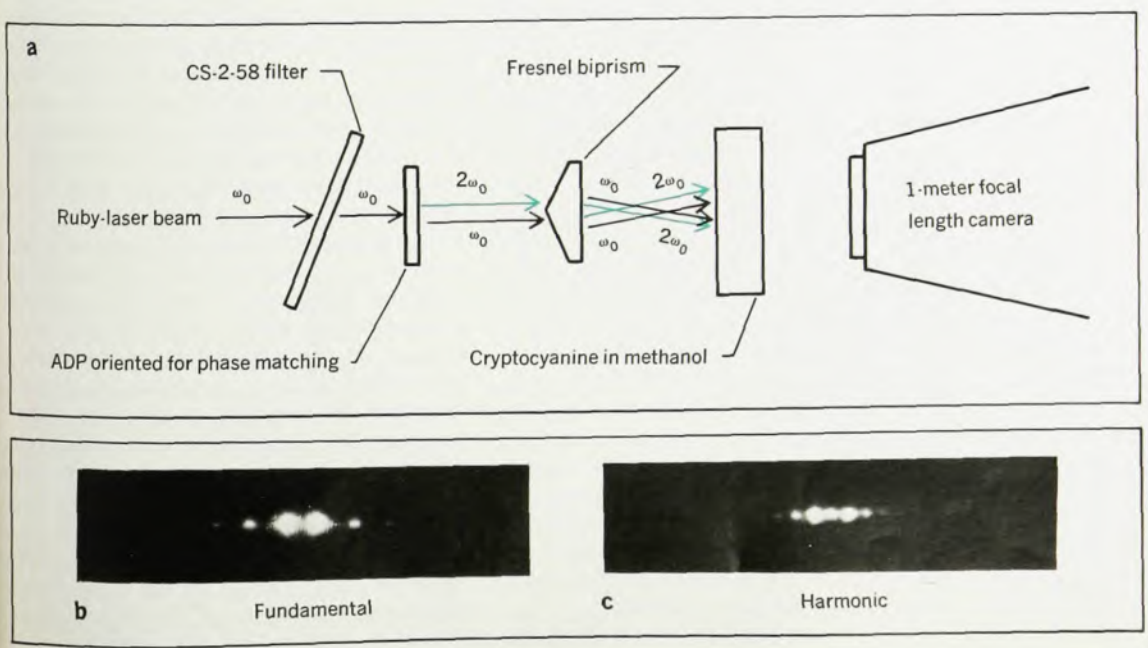

Four-beam experiment verifies grating model for thermal Rayleigh scattering. Optical arrangement (a) splits beam into four parts. The weak second-harmonic beams alone can not produce stimulated thermal scattering, but they are scattered in the presence of the more intense fundamental beams. The angular spacing for harmonic-beam scattering (c) is just half that for the fundamental (b), as the model predicts. Figure 6

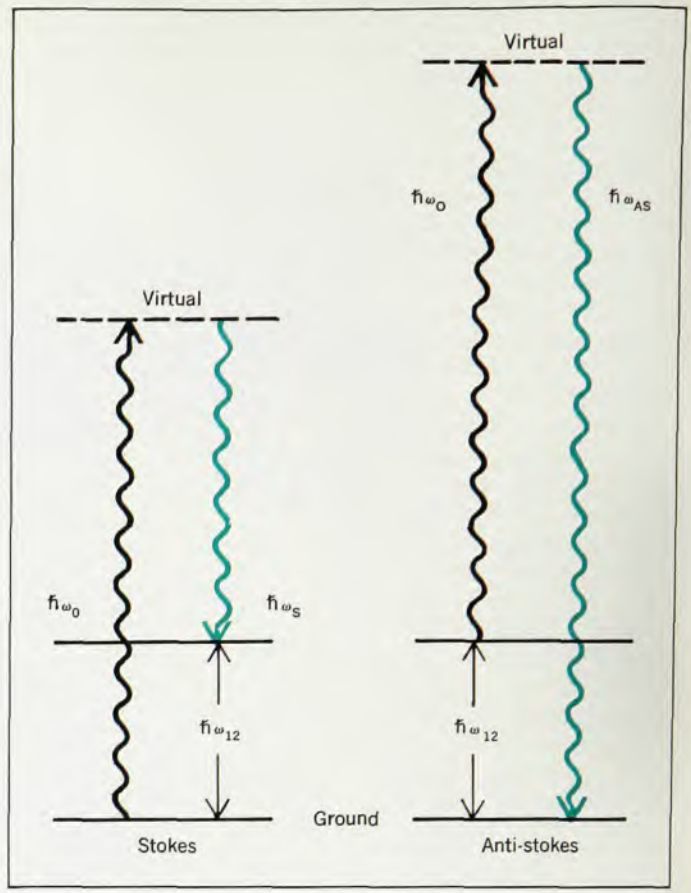

The two types of Raman scattering. In Stokes-type scattering (left) a photon with energy $\hbar\omega_0$, incident (black) on a ground-state molecule, excites the molecule to a (virtual) upper excited level. The molecule falls to a lower excited level, and the photon is scattered away (color) with energy $\hbar\omega_S < \hbar\omega_0$. In anti-Stokes scattering (right) the photon is incident (black) on an excited-state molecule, which falls back to the ground state after being raised to the upper excited state. The emitted photon (color) has energy $\hbar\omega_{AS} > \hbar\omega_0$. In both cases change in energy is $\hbar\omega_{12}$. Figure 7

ulated with picosecond laser pulses. Figure 8 shows results for methanol (CH_3OH). The spontaneous Raman spectrum in figure 8a shows two strong lines; a narrow one at 2837 cm^{-1}, corresponding to a CH stretching mode, and a broader one at 2942 cm^{-1}, corresponding to a CH_3 bending mode. The steady-state gain for the CH stretching-mode line is higher because of its high peak cross section, and in fact this is the only line observed with Q-switched pulse excitation. On the other hand the transient gain for the bending mode should be slightly larger than for the stretching mode, because the bending mode has a larger integrated cross section. Figure 8b shows that picosecond-pulse excitation stimulates both lines. Most probably the bending mode dominates at the beginning of the pulse, whereas the stretching mode dominates in the trailing edge.

Stokes pulsewidth measurements in liquids[20] and gases[21] confirm that the Stokes pulses generated by a mode-locked ruby laser are at least as short in duration as the exciting laser pulses, and the spectral linewidths are at least as broad. Very recently the Stokes-pulse time delay predicted by theory has been observed.[21]

Picosecond pulse excitation is also useful for discriminating between Raman scattering and more slowly responding competing gain processes, such as stimulated Brillouin scattering. This is particularly valuable in gases, because with Q-switched pulses Brillouin scattering is often the dominant nonlinearity, and Raman scattering is unobservable. With Q-switched lasers, stimulated vibrational Raman scattering has been observed only for methane, hydrogen and deuterium, and stimulated rotational scattering has been observed only in hydrogen and deuterium. With a mode-locked laser, on the other hand, stimulated vibrational and rotational scattering have been observed in a wide variety of gases.

Nonlinear optical effects

To observe nonlinear optical effects we need extremely high optical electric fields, and picosecond pulses have the highest fields obtainable. Certain nonlinear effects such as harmonic generation and multiple photon absorption are particularly interesting because they form the basis of the techniques used to measure ultrafast pulses. Other effects are important because with them we can alter the phase or amplitude structure of a pulse, or discriminate between pulses on the basis of their intensity or energy.

The lowest-order nonlinear effects are those produced by a polarization second order in the optical electric field. Included are second-harmonic generation, sum and difference frequency generation, parametric amplification and optical rectification. Although all these effects have been observed with Q-switched pulses, or pulses of even longer duration, some new features are introduced if we use picosecond-pulse excitation.

The most obvious difference is the increased strength of the interaction caused by the increased intensity of the pulse. The peak power of a simultaneously Q-switched and mode-locked pulse train exceeds that of a Q-switched pulse with the same energy and total duration by a factor equal to the duty cycle. We have assumed that the power in the fundamental beam is not depleted and that certain other conditions to be discussed later are met. This ratio is typically of the order of 10^3. Because the harmonic generation varies as the square of the intensity, we can expect increases of the order of 10^6–10^8 and similar increases in conversion efficiency can be obtained for the other second-order nonlinear processes.

Another new feature arises from the extremely short duration and correspondingly large spectral width of the pulses. For efficient conversion to occur in a process such as second-harmonic generation, the phase velocities of the fundamental and second-harmonic radiation must be equal; this condition is called "phase matching." Phase matching ensures that the induced nonlinear polarization has the proper spatial phase distribution to radiate in the forward direction. In a dielectric medium, dispersion generally prevents phase matching.

A common solution to this problem involves the use of birefringence. One of the radiation fields, fundamental or harmonic, is allowed to propagate as an ordinary wave and the other as an extraordinary wave. If the crystal is sufficiently birefringent, a propagation angle exists for which the phase-matching condition is met. As a result of dispersion, this angle is frequency dependent; for any given angle the conversion process $\omega \rightarrow 2\omega$ is phase matched for only one frequency. For a single mode or reasonably narrow-band Q-switched laser, this restriction is unimportant. Picosecond pulses, however, have an appreciable spectral width (for the neodymium-glass laser, for example, the width is of the order of one percent of the laser frequency) and the entire spectral width of the pulse can not be phase matched simultaneously. The resultant degradation in the conversion efficiency can outweigh the advantages gained by the increased power as well

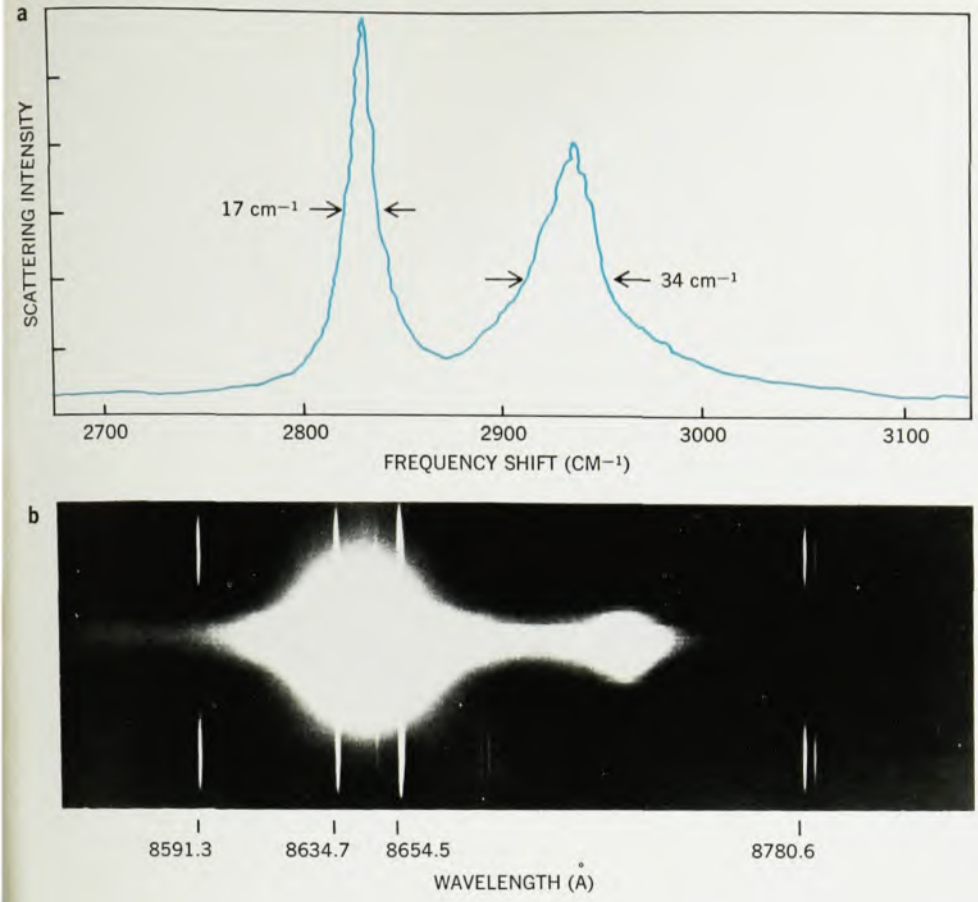

Spontaneous Raman spectrum of methanol (CH_3OH) shows (a) a narrow line at 2837 cm^{-1} (CH stretching) and a broader one at 2942 cm^{-1} (CH_3 bending). Only the narrower line, which has higher steady-state gain, is observed with Q-switched pulse excitation, but picosecond pulse excitation stimulates both lines (b).
Figure 8

as distort the pulse shape of the second-harmonic radiation.

Several authors have analyzed this problem.[22] A first-order correction for the broad spectral width leads to the very logical result that to convert short-pulse radiation efficiently we must match the group velocities of the fundamental and harmonic waves as well as their phase velocities. Spatial coincidence is then maintained between the fundamental pulse and the harmonic pulse it generates.

We can not in general satisfy both the phase and group-velocity matching requirements simultaneously for a given material. Once the propagation direction is chosen to satisfy the phase matching, the dispersive properties of the material determine the group-velocity mismatch. For this reason, the magnitude of the nonlinear coefficient is not the sole consideration in the selection of a material for harmonic generation. For example potassium dihydrogen phosphate (KDP) is a better material for generation of second-harmonic radiation from very short pulses of 1.06-micron radiation than lithium niobate ($LiNbO_3$) despite the larger nonlinear coefficient of the niobate.

If the group velocities are matched, the envelope of the second-harmonic pulse is the square of the envelope of the fundamental pulse, as is required if the second-harmonic generation is to be used in an intensity-correlation pulse-duration measurement. Because of the quadratic response the second-harmonic pulse is only about half as long as the fundamental pulse. Pulse shortening and lengthening due to mismatch have been observed experimentally.

We can treat parametric amplification of picosecond pulses similarly. The case that has received the most attention is the degenerate one for which the output (signal and idler) frequencies are both equal to one half the input (pump) frequency; this is the inverse of second-harmonic generation. For matched group velocities the subharmonic pulse travels along under the pumping pulse and experiences an exponential gain with a coefficient proportional to the amplitude of the pumping pulse; the sharpening is stronger here than for harmonic generation, because the gain is exponential rather than quadratic.

Optical rectification, a nonlinear process first observed as an induced dc voltage across a crystal of KDP during the passage of an intense ruby-laser pulse, can also be studied with picosecond pulses. The effect is usually difficult to observe because the resulting signal is of low voltage and short duration and is hard to distinguish from other spurious signals produced by acoustic and pyroelectric effects. If a periodic train of picosecond pulses propagates through a nonlinear crystal, optical rectification leads to a periodic voltage fluctuation across the crystal, which may be detected with a sensitive rf receiver tuned to any one of the harmonics of the pulse-repetition frequency. Harmonic signals as high as 10 GHz have been reported in KDP and $LiNbO_3$ with this technique.

When a picosecond pulse of limited spatial extent passes through a nonlinear dielectric, optical rectification leads to a polarization pulse that moves through the crystal with a velocity equal to the group velocity of the original optical pulse. We can regard the polarization as an equivalent moving-charge distribution. Because of dispersion there will be regions of the spectrum for which the phase velocity is less than the velocity of the polarization pulse; this is just the condition needed to generate Cerenkov radiation, and we would expect the moving polarization pulse to emit microwave radiation.

The next order of nonlinear effects are those caused by a polarization that is third order in the electric field. This type of nonlinearity gives rise to stimulated Rayleigh, Raman and Brillouin scattering (which we have already discussed), self-focusing of optical beams, the optical Kerr effect, third-harmonic generation and two-photon absorption. The use of picosecond pulses has helped to clarify some of the mechanisms responsible for self-focusing, which results from processes such as electrostriction (increased refractive index in a high-field region), molecular reorientation or electronic nonlinearities. The nonlinear changes in the refractive index caused by these processes have different characteristic times, so that by investigating the self-focusing for pulses of

different durations, we can determine the relative importance of the processes and establish the characteristic times.

Electrostriction is the slowest process and is probably ineffective even for nanosecond-long Q-switched pulses. The optical Kerr effect produced by molecular reorientation can have a much faster response time. Experiments to measure the self-focusing threshold by measuring the threshold for stimulated Raman scattering have been done and a marked decrease in Raman scattering, and presumably self-focusing, was observed with pulses shorter than the molecular-reorientation time.

Generating acoustic waves. The transient surface heating of materials by high-power picosecond laser pulses can produce intense and extremely short acoustic shocks. In an early experiment, a mode-locked neodymium-glass laser was used to irradiate a metal film deposited on the end of a bar of $LiNbO_3$.[23] The repetition rate of the laser was 200 MHz, the pulse lasted a few picoseconds, and the energy of each pulse was about one millijoule. The thermal stress produced when the metal film partially absorbed the radiation led to acoustic shocks that propagated down the crystal. As the shocks reflected off the opposite end of the crystal a piezoelectric voltage was generated and could be detected by a radio receiver tuned to one of the harmonics of the 200-MHz pulse repetition rate. When the output of the receiver was displayed on an oscilloscope, the sharpness of the tuning showed the sound was confined to harmonics of the pulse-repetition frequency. Signals were detected at frequencies as high as 10 GHz at room temperature. This technique is a convenient way of producing discrete sets of acoustic frequencies well into the microwave region and demonstrates the possibility of producing ultrashort acoustic pulses.

In a more recent experiment a single picosecond pulse excites an extremely intense stress wave in a quartz crystal.[24] The pulse, which lasts two to four picoseconds at an energy of 10–20 joules, is produced by amplification of a pulse selected from a mode-locked neodymium oscillator. The quartz crystal surface to be irradiated is plated with aluminum or aluminum and gold. Results show that the laser pulse generates a stress wave with a subnanosecond rise time, a half-width of about two nanoseconds and an amplitude in excess of ten kilobars.

Plasma studies. With the focused radiation from high-powered Q-switched lasers, high-density, high-temperature plasmas have been produced in gases, from solid surfaces and from single micron-sized solid particles. Researchers have also produced high-temperature plasmas with ultrafast pulses. (A bibliographical review of laser radiation interaction with solids is given by ref. 25.) The resulting plasmas have been used in fundamental studies of radiation–matter interactions, to excite high-temperature gas reactions, to produce extremely thin vapor-deposited coatings, as spectral sources for microanalysis and to study highly excited ions.

Laser methods can generate plasmas with a wide range of composition, density, ionization and temperature properties; laser-generated gas-breakdown plasmas, for example, can have electron densities greater than 10^{19} cm^{-3} and temperatures exceeding 100 eV. In the solid surface plasma plumes very highly ionized atoms can be obtained. Single high-energy ultrafast pulses have been used to generate thermonuclear-neutron emission from lithium-deuteride surfaces, and picosecond pulses have been used to investigate the influence of laser-mode interference and optical breakdown threshold in gases and optical self-focusing effects in plasmas.

Recently carbon-dioxide lasers at atmospheric pressure emitting pulses that last from 10^{-7} sec down to 6×10^{-9} sec have been developed, offering additional interesting possibilities for generating and investigating high-temperature plasmas.

Other uses for ultrafast pulses, such as ranging experiments, optical radar, optical data processing and communications are possible. For them to be practical however, we need ultrafast electronic equipment to interface with the optical systems.

References

1. R. W. Hellwarth in *Lasers* (A. K. Levine, ed.), Marcel Dekker, New York, 1966, page 243.
2. E. B. Treacy, Phys. Lett. **28A,** 34 (1968); N. G. Basov, P. G. Kriukov, S. D. Zakharov, Yu. V. Senatsky, S. V. Tchekalin, IEEE J. Quant. Elect. **QE-4,** 864 (1968); A. J. DeMaria, R. Gagosz, H. A. Heynau, A. W. Penney Jr, G. Wisner, J. Appl. Phys. **38,** 2413 (1967); G. W. Gobeli, J. C. Bushnell, P. S. Peercy, E. D. Jones, Phys. Rev. **188,** 300 (1969).
3. D. A. Stetser, A. J. DeMaria, Appl. Phys. Lett. **9,** 118 (1966).
4. L. E. Hargrove, R. L. Fork, M. A. Pollack, Appl. Phys. Lett. **5,** 4 (1964); M. H. Crowell, IEEE J. Quant. Elect. **QE-1,** 12 (1965).
5. A. J. DeMaria, W. H. Glenn, M. J. Brienza, M. E. Mack, Proc. IEEE **57,** 1 (1969).
6. J. A. Armstrong, Appl. Phys. Lett. **10,** 16 (1967); H. P. Weber, Phys. Lett. **27A,** 321 (1968); W. H. Glenn, M. J. Brienza, Appl. Phys. Lett. **10,** 221 (1967); M. Maier, W. Kaiser, J. A. Giordmaine, Phys. Rev. Lett. **17,** 1275 (1966).
7. W. Szymanowski, Z. Physik **35,** 450 (1935); P. Pringsheim, *Fluorescence and Phosphorescence,* Interscience, New York, 1949, page 10.
8. W. H. Glenn, M. J. Brienza, A. J. De Maria, Appl. Phys. Lett. **12,** 54 (1968).
9. M. E. Mack, J. Appl. Phys. **39,** 2483 (1968).
10. M. A. Duguay, J. W. Hansen, Optics Commun. **1,** 254 (1969).
11. M. A. Duguay, J. W. Hansen, Appl. Phys. Lett. **15,** 192 (1969).
12. J. W. Shelton, J. A. Armstrong, IEEE J. Quant. Elect. **3,** 696 (1967); R. I. Scarlet, J. F. Figueria, H. Mahr, Cornell Univ. Lab. of Atomic and Solid State Physics Tech. Rept. 24, May 1968.
13. K. B. Eisenthal; K. H. Drexhage, J. Chem. Phys. **51,** 5720 (1969).
14. P. M. Rentzepis, Chem. Phys. Lett. **2,** 117 (1968).
15. P. M. Rentzepis, M. R. Topp, R. P. Jones, J. Jortner, Phys. Rev. Lett. **25,** 1742 (1970).
16. R. M. Herman; M. A. Gray, Phys. Rev. Lett. **19,** 824 (1967); D. H. Rank, C. W. Cho, N. D. Foltz, T. A. Wiggins, Phys. Rev. Lett. **19,** 828 (1967); G. I. Zaitsev, Yu. I. Kyzylasov, V. S. Starunov, I. I. Fabelinskii, JETP Lett. **6,** 255 (1967).
17. M. E. Mack, Phys. Rev. Lett. **22,** 13 (1969).
18. M. E. Mack, Ann. New York Acad. Sci. **168,** 419 (1970).
19. C. S. Wang, Phys. Rev. **182,** 482 (1969); R. L. Carman, F. Shimizu, C. S. Wang, N. Bloembergen, Phys. Rev. **A2,** 60 (1970).
20. R. L. Carman, M. E. Mack, F. Shimizu, N. Bloembergen, Phys. Rev. Lett. **23,** 1327 (1969).
21. R. L. Carman, F. Shimizu, J. Reintjes, N. Bloembergen, M. E. Mack, *Proceedings* of the 1970 International Quantum Electronics Conference, Kyoto, Japan.
22. J. Comly, E. Garmire, Appl. Phys. Lett. **12,** 7 (1968); R. C. Miller, Phys. Lett. **26A,** 177 (1968); W. H. Glenn, IEEE J. Quant. Elect. **QE-5,** 284 (1969); S. A. Akhmanov, A. S. Chirkin, K. N. Drabovitch, A. I. Kovrigin, R. V. Khokhlov, A. P. Sukhorokov, IEEE J. Quant. Elect. **QE-4,** 598 (1968); S. L. Shapiro, Appl. Phys. Lett. **13,** 19 (1968).
23. M. J. Brienza, A. J. DeMaria, Appl. Phys. Lett. **11,** 44 (1967).
24. P. S. Peercy, E. D. Jones, J. C. Bushnell, G. W. Gobeli, Appl. Phys. Lett. **16,** 120 (1970).
25. C. DeMichelis, IEEE J. Quant. Elect. **QE-6,** 630 (1970). □